

# Release of Fibrinopeptides by the Slow and Fast Forms of Thrombin<sup>†</sup>

Alessandro Vindigni and Enrico Di Cera\*

Department of Biochemistry and Molecular Biophysics, Washington University School of Medicine, Box 8231, St. Louis, Missouri 63110

Received November 30, 1995; Revised Manuscript Received February 1, 1996<sup>⊗</sup>

**ABSTRACT:** The release of fibrinopeptides A and B by the slow and fast forms of thrombin was studied over the temperature range from 5 to 45 °C and the salt concentration range from 100 to 800 mM. The sequential mechanism for the release of fibrinopeptides originally proposed by Shafer was found to be obeyed under all conditions examined. The origin of preferential binding of fibrinogen and fibrin I to the fast form of thrombin in the transition state is in the second-order rate constant for association,  $k_1$ . In the case of fibrinogen, the values of  $k_1$  for interaction with the fast and slow forms at 25 °C are  $19 \pm 4$  and  $2.5 \pm 0.3 \mu\text{M}^{-1} \text{s}^{-1}$ , with an activation energy of about 10 kcal/mol in both forms. In the case of fibrin I, the analogous values of  $k_1$  are  $9.1 \pm 0.7$  and  $2.5 \pm 0.2 \mu\text{M}^{-1} \text{s}^{-1}$ , and the activation energy is about 4.5 kcal/mol in both forms. The mechanism of recognition of fibrinogen and fibrin I by thrombin entails a diffusion-controlled step with a small energy barrier. Analysis of the temperature dependence of the coupling free energy for allosteric switching indicates that the preferential interaction of fibrinogen and fibrin I with the fast form of thrombin in the transition state is entropy-driven, signaling a contribution of the hydrophobic effect to the slow  $\rightarrow$  fast transition. The salt dependence of the release of fibrinopeptides shows a constant coefficient  $\Gamma_{\text{salt}} = d \ln(k_{\text{cat}}/K_m)/d \ln [\text{salt}]$  in the concentration range examined. Interestingly, the value of  $\Gamma_{\text{salt}}$  is independent of the salt used (NaCl, ChCl, or NaF) and is  $-1.5 \pm 0.1$  for fibrinopeptide A and  $-2.5 \pm 0.1$  for fibrinopeptide B. Hence,  $\Gamma_{\text{salt}}$  reflects predominantly the electrostatic contribution to the formation of the transition state, with a larger contribution seen in the interaction of thrombin with fibrin I. It is concluded that the interaction of thrombin with fibrinogen and fibrin I, leading to the release of fibrinopeptides A and B, is driven by electrostatic forces that presumably favor the correct preorientation of the enzyme and the substrate to form a productive complex in the transition state. This electrostatic-steering effect, also reported for thrombin–hirudin interaction, leads to a diffusion-controlled encounter with a very small energy barrier. Once the complex is formed, the enzyme switches to the fast form as a result of entropic factors presumably linked to water release from a more extended surface of recognition. While the release of fibrinopeptides as a function of salt concentration was being studied, an important observation was made on the role of  $\text{Cl}^-$  in the formation of the fibrin clot. This anion drastically and specifically reduces the thickness of fibrin fibers, as judged by the 10-fold decrease in the equilibrium turbidity of clots developed in NaCl as compared to the turbidity of clots developed in NaF. Hence, the transition from a “coarse” to a “fine” clot induced by an increase in ionic strength as first described by Ferry is, instead, due to the specific binding of  $\text{Cl}^-$  to intermediates in the ensuing polymerization. In fact, no change in the clotting curve is observed when the ionic strength is changed with NaF.

Fibrinogen circulates in the plasma as a dimer of three chains,  $(\text{A}\alpha\text{B}\beta\gamma)_2$ , that are covalently linked by disulfide bonds (Doolittle, 1984; Binnie & Lord, 1993). This molecule is converted into the insoluble fibrin clot by a series of enzymatic and physical steps that conclude the procoagulant pathway of the blood coagulation cascade. Important aspects of the physical steps have been unraveled in a number of careful studies (Ferry & Morrison, 1947; Shulman et al., 1953; Sturtevant et al., 1955; Hageman & Scheraga, 1977; Hantgan & Hermans, 1979; Wilf & Minton, 1986; Mihalyi, 1988; Mihalyi et al., 1991). Understanding of the enzymatic steps has been greatly facilitated by HPLC<sup>1</sup> analysis of the release of fibrinopeptides (Martinelli & Scheraga, 1980; Higgins et al., 1983; Hofsteenge et al., 1986) and by measurements of the equilibrium dissociation constant for

thrombin–fibrinogen interaction (Hopfner & Di Cera, 1992). Structural information on the recognition of fibrinogen by thrombin has begun to emerge (Martin et al., 1992; Stubbs et al., 1992), along with important details on its site-specific molecular components (Guinto et al., 1995).

The precise sequence of thrombin-catalyzed events leading to clot formation has been elucidated by Shafer (Higgins et al., 1983; Lewis et al., 1985; Ng et al., 1993). The Shafer mechanism states that fibrinogen cleavage by thrombin encompasses four steps. First, a highly specific cleavage at the  $\text{A}\alpha$  chain leads to release of fibrinopeptide A (FpA) and formation of fibrin I monomers. Second, these monomers aggregate to form fibrin I protofibrils. Third, a second highly specific cleavage by thrombin at the  $\text{B}\beta$  chain of the fibrin I monomers leads to release of fibrinopeptide B (FpB) and formation of fibrin II protofibrils. Fourth, these protofibrils

<sup>†</sup> This work was supported in part by NIH Research Grant HL49413 and by a grant from the American Heart Association. E.D.C. is an Established Investigator of the American Heart Association and Genentech. A.V. is a William M. Keck Fellow.

\* Address correspondence to this author.

<sup>⊗</sup> Abstract published in *Advance ACS Abstracts*, March 15, 1996.

<sup>1</sup> Abbreviations: Ch, choline; FpA, fibrinopeptide A; FpB, fibrinopeptide B; GuHCl, guanidine hydrochloride; HPLC, high-performance liquid chromatography; PEG, poly(ethylene glycol); Tris, tris(hydroxymethyl)aminomethane.

rapidly aggregate to form the scaffold of the fibrin clot. This mechanism accounts for clot formation under physiological conditions and provides a useful framework for understanding the procoagulant role of thrombin in the coagulation cascade. This mechanism, however, has never been put to a systematic experimental test by characterization of the release of fibrinopeptides as a function of temperature or salt concentration. The importance of such studies, recognized by Shafer himself (Ng et al., 1993), stems from the need to identify the physical driving forces for thrombin–fibrinogen interaction that lead to clot formation. Specifically, temperature studies reveal the enthalpic and entropic components linked to formation of the transition state and analysis of the salt dependence provides important information on specific (site binding) and nonspecific (electrostatic) components.

A more important reason for undertaking such systematic analysis is that previous studies of thrombin–fibrinogen interaction have been carried out without taking into account the allosteric nature of the enzyme and its control by  $\text{Na}^+$ . Under physiological concentrations of NaCl (145 mM), at 37 °C, thrombin is equally partitioned between the slow and fast forms (Wells & Di Cera, 1992) that differ in their ability to bind fibrinogen (Mathur et al., 1993) and release the fibrinopeptides (Dang et al., 1995). A quantitative understanding of the physicochemical aspects of the release of fibrinopeptides, as well as of any other physiologically relevant aspect of thrombin function like the interaction with thrombomodulin, protein C, antithrombin, and heparin, necessarily demands the contribution of the allosteric forms of the enzyme to be sorted out. In this study, we report on the properties of the slow and fast forms of thrombin in their interaction with fibrinogen, characterize the enzymatic steps of fibrinopeptide release, and test the Shafer mechanism over the temperature range from 5 to 45 °C and the salt concentration from 100 to 800 mM. The results of similar studies on the interaction of thrombin with thrombomodulin and antithrombin will be discussed elsewhere. We also describe an important and unanticipated effect of  $\text{Cl}^-$  in the formation of the fibrin clot, which offers a re-interpretation of the well known transition from a “coarse” to a “fine” clot as first described by Ferry (Ferry & Morrison, 1947).

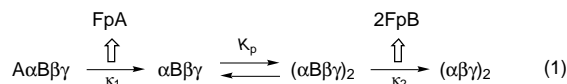
## MATERIALS AND METHODS

Human  $\alpha$ -thrombin was purified and tested for activity as described (Wells & Di Cera, 1992; Dang & Di Cera, 1994). Human fibrinogen of the highest purity and activity was purchased from Hematologic Technologies, Inc. (Essex Junction, VT) and was further purified and tested for activity as described (De Cristofaro & Di Cera, 1991, 1992; Mathur et al., 1993). The slow and fast forms of thrombin were studied under experimental conditions of 5 mM Tris, 0.1% PEG, and pH 8.0, over the temperature range from 5 to 45 °C. The ionic strength was kept constant at 200 mM with NaCl when the fast form was being studied or with ChCl when the slow form was being studied. The pH was precisely adjusted at room temperature to obtain the value of 8.0 at the desired temperature. Tris buffer has a  $\text{p}K_a = 8.06$  at 25 °C and a temperature coefficient of  $\Delta\text{p}K_a/\Delta T = -0.027$  (Stoll & Blanchard, 1990). These properties ensured buffering over the entire temperature range examined. Measurements of the pH dependence of fibrinogen binding to thrombin over the pH range from 6.0 to 10.0 show

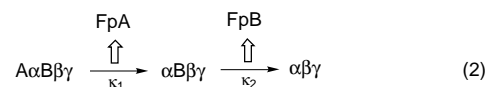
negligible changes around pH 8.0 (Mathur et al., 1993), so negligible or no contribution from linked proton exchange is to be expected under the experimental conditions used. The stability of thrombin was checked over the entire temperature range examined, as described (Ayala et al., 1995).

The release of FpA and FpB by the slow and fast forms of thrombin was quantified from analysis of progress curves as described (Ng et al., 1993; Dang et al., 1995), using eq 3 and also KINSIM and FITSIM (Barshop et al., 1983; Zimmerle & Frieden, 1989). Solutions of thrombin and fibrinogen were incubated under the desired solution conditions of salt concentration and temperature to allow for equilibration. The active thrombin concentration ranged from 0.2 to 10.0 nM. Fibrinogen was used at concentrations of 0.2  $\mu\text{M}$ , well below the estimated value of  $K_m$  (see below). The reaction, started by addition of thrombin to the fibrinogen solution, was quenched at different time intervals with 3 M perchloric acid. The sample was then centrifuged at 10000g for 8 min, and the supernatant was analyzed by reverse-phase HPLC, using a Waters 717plus Autosampler for 1 mL injections into the HPLC system equipped with a Waters  $\text{C}_{18}$  column (4.6  $\times$  250 mm). Elution was carried out at a flow rate of 1 mL/min, with a gradient containing 80 mM sodium phosphate buffer at pH 3.1 (solvent A) and acetonitrile (solvent B). Optimal separation was obtained using 17% of solvent B from 0 to 15 min, followed by a 10 min linear gradient to 40% of solvent B. The effluent was monitored at 205 nm. Extinction coefficients for FpA and FpB were derived by calibration and quantitative amino acid analysis of highly pure standards (Dang et al., 1995).

The time course of FpA and FpB release was analyzed according to the sequential mechanism of Shafer (Higgins et al., 1983; Lewis et al., 1985; Ng et al., 1993)



The mechanism in scheme 1 assumes that FpA is released from fibrinogen to form fibrin I with a rate constant of  $\kappa_1$ . Fibrin I aggregates with an association constant  $K_p$  to form protofibrils I, from which FpB is released with a rate constant of  $\kappa_2$ . Under conditions where the concentration of fibrinogen is small compared to  $K_m$ ,  $\kappa_1$  and  $\kappa_2$  are the same as the specificity constant  $k_{\text{cat}}/K_m$  times the active enzyme concentration,  $e_T$ . If the aggregation step is fast compared to all other rates, which is the case at thrombin concentrations that are rate-limiting (Lewis et al., 1985), scheme 1 contracts into the following simpler scheme



The time dependence of [FpA] and [FpB] is given by

$$[\text{FpA}] = [\text{FpA}]_\infty [1 - \exp(-\kappa_1 t)] \quad (3a)$$

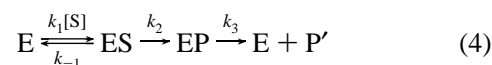
$$[\text{FpB}] =$$

$$f[\text{FpA}]_\infty \left[ 1 + \frac{\kappa_2}{\kappa_1 - \kappa_2} \exp(-\kappa_1 t) - \frac{\kappa_1}{\kappa_1 - \kappa_2} \exp(-\kappa_2 t) \right] \quad (3b)$$

The factor  $f < 1$  reflects the incomplete recovery of FpB due to trapping by the clot. Since an incomplete recovery of FpB was observed systematically under all conditions reported in this study, with wild-type thrombin and several mutants (Guinto et al., 1995), and was also documented by others (Higgins et al., 1985; Martinelli & Scheraga, 1980; Hofsteenge et al., 1986; Mihalyi, 1988) without an explanation being provided, a careful analysis was undertaken to clarify its possible origin. An incomplete release of FpB could underlie an alternative kinetic pathway leading to clot formation that is independent of the release of FpB. This possibility is supported by the observation that reptilase only cleaves the A $\alpha$  chain of fibrinogen and nonetheless induces clot formation (Hantgan & Hermans, 1979). Extension of the kinetic mechanism 2 to include an alternative pathway to clot formation is straightforward. The expression for [FpA] in eq 3a remains unchanged, while the rate constant  $\kappa_2$  in eq 3b becomes a linear combination of the specificity constant for FpB release and the rate constant pertaining to the alternative pathway. On the other hand, an incomplete release of FpB could be an artifact of the assay and specifically result from an entrapment by the ensuing clot when the reaction is quenched with perchloric acid. A fraction of FpB could then be lost during centrifugation prior to the sample being loaded into the HPLC. The former possibility was evaluated by studies of the dependence of the kinetic rate constants  $\kappa_1$  and  $\kappa_2$  in eqs 3a,b on the thrombin concentration  $e_T$ . A linear dependence of these terms on  $e_T$  was observed, in agreement with previous findings (Higgins et al., 1983; Ng et al., 1993), thereby excluding a pathway to clot formation independent of thrombin concentration. Experiments carried out to evaluate the possibility that fractions of FpB could be trapped in the ensuing polymerization and coprecipitate with the clot prior to HPLC analysis revealed that the total expected amount of FpB could be recovered by dissolving the clot in 8 M urea, or 6 M GuHCl, and then loading the whole sample into the HPLC without prior centrifugation. Loading pure FpB into the HPLC after treatment with acid and centrifugation always yielded the total expected amount of FpB. This was also the case in the presence of thrombin or fibrinogen. Only when both thrombin and fibrinogen were present was the amount of total FpB released less than expected. The amount of FpB trapped by the clot was found to be proportional to the amount released, regardless of solution conditions, as judged by control experiments of clot formation in the presence of variable amounts of added FpB. Hence, eq 3b was used to analyze the progress curves of FpB release, with the factor  $f$  reflecting the loss during centrifugation of the sample.

The validity of the assumptions embodied by eqs 3a,b was tested with KINSIM and FITSIM. These programs allow for simulation and fitting of progress curves to arbitrary kinetic mechanisms, with the rate equations integrated numerically. In all cases, the results derived by FITSIM agreed with the analysis based on eqs 3a,b. Determinations of FpA were also carried out as a function of fibrinogen concentration to derive initial velocities for analysis in terms of the Michaelis–Menten equation (Lewis et al., 1985). These measurements yielded independent determinations of  $K_m$  and  $k_{cat}$  for the interaction of fibrinogen with the slow and fast forms of thrombin.

The value of  $k_{cat}/K_m$  derived from analysis of progress curves of FpA and FpB release conveys little information on the molecular origin of specificity based on the mechanism of hydrolysis of amide bonds. However, the temperature dependence of the specificity constant may be revealing of changes in rate-limiting steps and allows for resolution of individual kinetic rate constants under certain conditions. In the specific case of the release of FpA and FpB, the second-order rate constant for thrombin interaction with fibrinogen and fibrin I can be determined. This parameter provides important details on the mechanism of interaction. The mechanism of hydrolysis of amide bonds by serine proteases is



where  $k_2$  and  $k_3$  are the acylation and deacylation rate constants, while  $k_1$  and  $k_{-1}$  are the rate constants for binding and dissociation of the substrate, S. The deacylation rate constant also includes the rate constant of product diffusing away from the active site, whichever is rate-limiting. The specificity constant depends on the individual rate constants as follows

$$\frac{k_{cat}}{K_m} = \frac{k_1 k_2}{k_{-1} + k_2} = k_1 \frac{\alpha}{1 + \alpha} \quad (5)$$

and is independent of the deacylation rate constant. The parameter  $\alpha$  measures the stickiness of the substrate (Cleland, 1977), which is the tendency to undergo acylation relative to dissociation back into the solution. It follows from eq 5 that the specificity constant always underestimates the second-order rate constant for formation of the enzyme–substrate complex and that the approximation is particularly inaccurate for poor substrates, or whenever  $\alpha \ll 1$ . The temperature dependence of the rate constants in eq 5 can be found from integration of the Arrhenius equation assuming a constant activation energy as

$$k_j = k_{j,0} \exp \left[ -\frac{E_j}{R} \left( \frac{1}{T} - \frac{1}{T_0} \right) \right] \quad (6)$$

where  $E_j$  is the activation energy associated with the rate constant  $k_j$ ,  $R$  is the gas constant,  $T$  is the absolute temperature, and  $k_{j,0}$  is the value of  $k_j$  at the reference temperature  $T_0 = 298.15$  K. Substitution into eq 5 yields

$$\frac{k_{cat}}{K_m} = k_{1,0} \exp \left[ -\frac{E_1}{R} \left( \frac{1}{T} - \frac{1}{T_0} \right) \right] \frac{\alpha_0 \exp \left[ \frac{E_\alpha}{R} \left( \frac{1}{T} - \frac{1}{T_0} \right) \right]}{1 + \alpha_0 \exp \left[ \frac{E_\alpha}{R} \left( \frac{1}{T} - \frac{1}{T_0} \right) \right]} \quad (7)$$

where  $E_\alpha = E_{-1} - E_2$ . The temperature dependence of the specificity constant is, in essence, the temperature dependence of  $k_1$  in the range where  $\alpha \gg 1$ . In this range, a plot of  $\ln(k_{cat}/K_m)$  vs  $1/T$  yields a straight line with the slope  $-E_1/R$ , from which the values of  $k_{1,0}$  and  $E_1$  can be estimated. Since the activation energies are all positive, the temperature dependence of the specificity constant is set by the difference

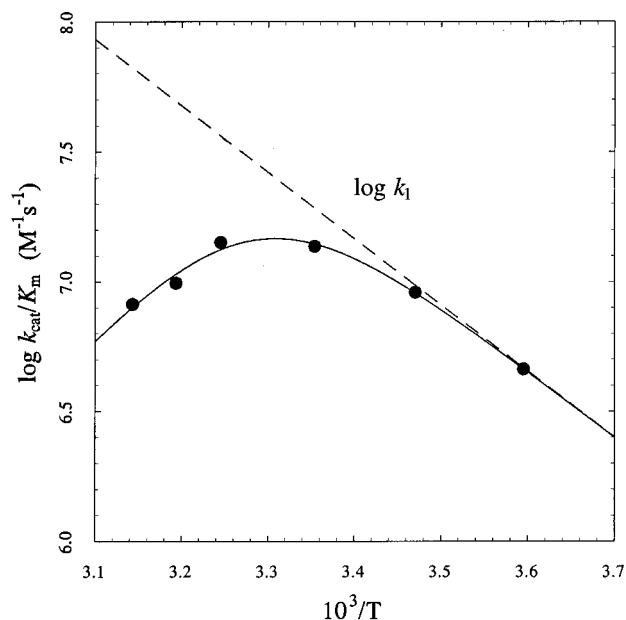


FIGURE 1: Arrhenius plot of the specificity constant for FpA release by the fast form of thrombin in the temperature range from 5 to 45 °C. Experimental conditions were as follows: 5 mM Tris, 0.1% PEG, pH 8.0, and 0.2 M NaCl. The continuous line was drawn according to eq 7 in the text, with best-fit parameter values listed in Table 2. The discontinuous line depicts the temperature dependence of the logarithm of  $k_1$ , which is derived from the specificity constant  $k_{\text{cat}}/K_m$  in the limit where  $\alpha \gg 1$  (see eqs 5 and 7). The curvature in the plot allows for resolution of the four independent parameters in eq 7 and provides information on the second-order rate constant for formation of the thrombin–fibrinogen complex, the parameter of stickiness, and the relevant activation energies.

$E_\alpha - E_1$ . This quantity is expected to be large and positive, since the energy barrier associated with substrate dissociation ( $E_{-1}$ ) is usually much larger than that for substrate binding ( $E_1$ ) or acylation ( $E_2$ ). In this case, the plot of  $\ln(k_{\text{cat}}/K_m)$  vs  $1/T$  has a distinct maximum, as shown in Figure 1. Processes with a low activation energy (e.g., substrate acylation) predominate at low temperatures, and therefore, the substrate becomes very sticky as  $1/T$  increases. In this range, the specificity constant becomes identical to  $k_1$ . At high temperatures, the process with the higher activation energy (e.g., substrate dissociation) is favored and the value of  $\alpha$  decreases progressively, making the specificity constant deviate from the straight line in Figure 1. The data in Figure 1 contain enough information to yield all four parameters in eq 7. Hence, analysis of the temperature dependence of  $k_{\text{cat}}/K_m$  yields the value of  $k_1$  and the ratio  $k_2/k_{-1}$  at any temperature, along with important information on the physical steps of formation of the enzyme–substrate complex and the parameter of stickiness.

The salt dependence of the specificity constant for the release of FpA and FpB was studied in the concentration range from 100 to 800 mM when using NaCl and ChCl and from 200 to 500 mM when using NaF. The data plotted as  $\ln(k_{\text{cat}}/K_m)$  vs  $\ln[\text{salt}]$  were fitted to a straight line according to the expression

$$\ln\left(\frac{k_{\text{cat}}}{K_m}\right) = A_0 + \Gamma_{\text{salt}} \ln[\text{salt}] \quad (8)$$

This is essentially the Taylor expansion of the function  $\ln(k_{\text{cat}}/K_m)$  around the logarithm of  $[\text{salt}] = 1$  M, where  $\ln$

$(k_{\text{cat}}/K_m) = A_0$ .  $\Gamma_{\text{salt}}$  is the phenomenological coefficient quantifying the change in  $\ln(k_{\text{cat}}/K_m)$  due to a change in  $\ln[\text{salt}]$  and represents the transition state analogue of the preferential interaction coefficient at equilibrium (Record et al., 1978; Record & Anderson, 1995). The value of  $\Gamma_{\text{salt}}$  depends on specific salt effects reflecting the net balance of ions exchanged when the enzyme and substrate form the transition state. In addition, the value of  $\Gamma_{\text{salt}}$  depends on purely electrostatic-screening effects of ions on protein domains that are involved in the formation of the transition state. Specific and nonspecific salt effects can be sorted out by measurement of the value of  $\Gamma_{\text{salt}}$  with salts containing components that differ widely in properties like hydration energies and ionic radii (Suelter, 1974; Collins & Washabaugh, 1985; Collins, 1995). Replacement of  $\text{Na}^+$  with the bulky cation  $\text{Ch}^+$  sheds light on specific cation binding effects, while the replacement of  $\text{Cl}^-$  with the more hydrated  $\text{F}^-$  unravels specific anion binding effects. Although different ions have different activity coefficients, these replacements do not affect the ionic strength of the solution in the salt concentration range examined (Collins & Washabaugh, 1985). A similar strategy has been used previously for thrombin (Wells & Di Cera, 1992; Ayala & Di Cera, 1994) and other systems (von Hippel & Wong, 1965; Lu & Draper, 1994; Overman & Lohman, 1994; Kenar et al., 1995).

Clotting curves were measured as described (De Cristofaro & Di Cera, 1991), by following the increase in turbidity at 350 nm as a function of time.

## RESULTS

Previous studies indicated that the fast form of thrombin releases FpA from fibrinogen and FpB from fibrin I with higher specificity (Dang et al., 1995). In the case of FpA, the fast form is nearly 10 times more specific at 25 °C. In order to identify the origin of this difference, the values of  $K_m$  and  $k_{\text{cat}}$  for thrombin–fibrinogen interaction were determined separately. The Michaelis–Menten curves for thrombin–fibrinogen interaction are shown in Figure 2, and the best-fit parameter values are summarized in Table 1. The higher specificity of the fast form is due to a higher  $k_{\text{cat}}$  and a lower  $K_m$ , consistent with previous studies (Mathur et al., 1993; Lord et al., 1995) and the results observed with chromogenic substrates (Wells & Di Cera, 1992). The specificity constant derived from these measurements is in good agreement with that determined independently from analysis of progress curves.

The release of fibrinopeptides by the slow and fast forms of thrombin was studied over the temperature range 5–45 °C to identify changes in rate-limiting steps and activation energies linked to formation of the thrombin–fibrinogen and thrombin–fibrin I complexes. These studies were also carried out to derive the second-order rate constant  $k_1$  for the interaction of the slow and fast forms of thrombin with fibrinogen and fibrin I, in order to better characterize the molecular origin of the higher specificity of the fast form. Typical progress curves of FpA and FpB release are given in Figure 3. Release of FpA precedes that of FpB, which is observed after a lag time. The release of FpB reaches a lower asymptote compared to that of FpA, due to entrapment by the clot (see Materials and Methods).

Analysis of progress curves using eqs 3a,b yields the specificity constants for FpA and FpB release. Figure 4

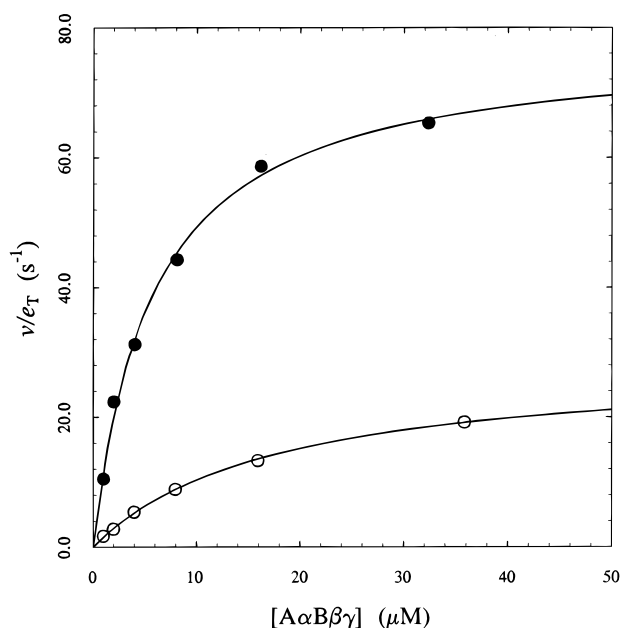


FIGURE 2: Michaelis–Menten curves for the interaction of the slow and fast forms of thrombin with fibrinogen. Experimental conditions were as follows: 5 mM Tris, 0.1% PEG, pH 8.0, 25 °C, and 0.2 M NaCl for the fast form (●) or 0.2 M ChCl for the slow form (○). Continuous lines were drawn according to the Michaelis–Menten equation, with best-fit parameter values listed in Table 1. The fast form cleaves fibrinogen and releases FpA with higher specificity because of a smaller  $K_m$  and a higher  $k_{cat}$  compared to those of the slow form.

Table 1: Michaelis–Menten Parameters for the Interaction of Fibrinogen with the Slow and Fast Forms of Thrombin, Leading to Release of FpA

	$K_m$ ( $\mu\text{M}$ )	$k_{cat}$ ( $\text{s}^{-1}$ )	$k_{cat}/K_m$ ( $\mu\text{M}^{-1} \text{s}^{-1}$ )	$k_{cat}/K_m$ ( $\mu\text{M}^{-1} \text{s}^{-1}$ ) <sup>a</sup>
fast	$5.7 \pm 0.5$	$77 \pm 2$	$13.5 \pm 0.9$	$13.7 \pm 0.2$
slow	$17.7 \pm 0.8$	$29 \pm 1$	$1.6 \pm 0.1$	$1.91 \pm 0.04$

<sup>a</sup> Value determined independently from analysis of progress curves of FpA release.

shows the results of measurements carried out as a function of temperature. The data yield the second-order rate constant  $k_1$  for fibrinogen and fibrin I monomer interaction with thrombin, as well as the activation energies  $E_1$  and  $E_\alpha$  and the parameter of stickiness,  $\alpha$ . The values of these parameters are listed in Table 2. The value of  $k_1$  for thrombin–fibrinogen interaction is larger in the fast form by a factor of 7, and this explains entirely the higher specificity of the fast form. The active site of the enzyme is clearly more accessible in this form, which is consistent with findings from small chromogenic substrates (Wells & Di Cera, 1992). In both forms, the formation of a productive complex between fibrinogen and thrombin requires a small activation energy, indicating that the process is diffusion-limited. The parameter of stickiness indicates that fibrinogen is a sticky substrate for thrombin and that, once the Michaelis–Menten complex is formed, the tendency of the reaction is to proceed in the direction of the chemical conversion of the acyl enzyme. There is no significant difference in the two forms in either the parameter of stickiness or the activation energy associated with it. The value of  $E_\alpha$  is very large and points out the significant differences in the activation energy for substrate dissociation and acylation. Once the thrombin–fibrinogen complex is formed, there is a very high energy barrier for

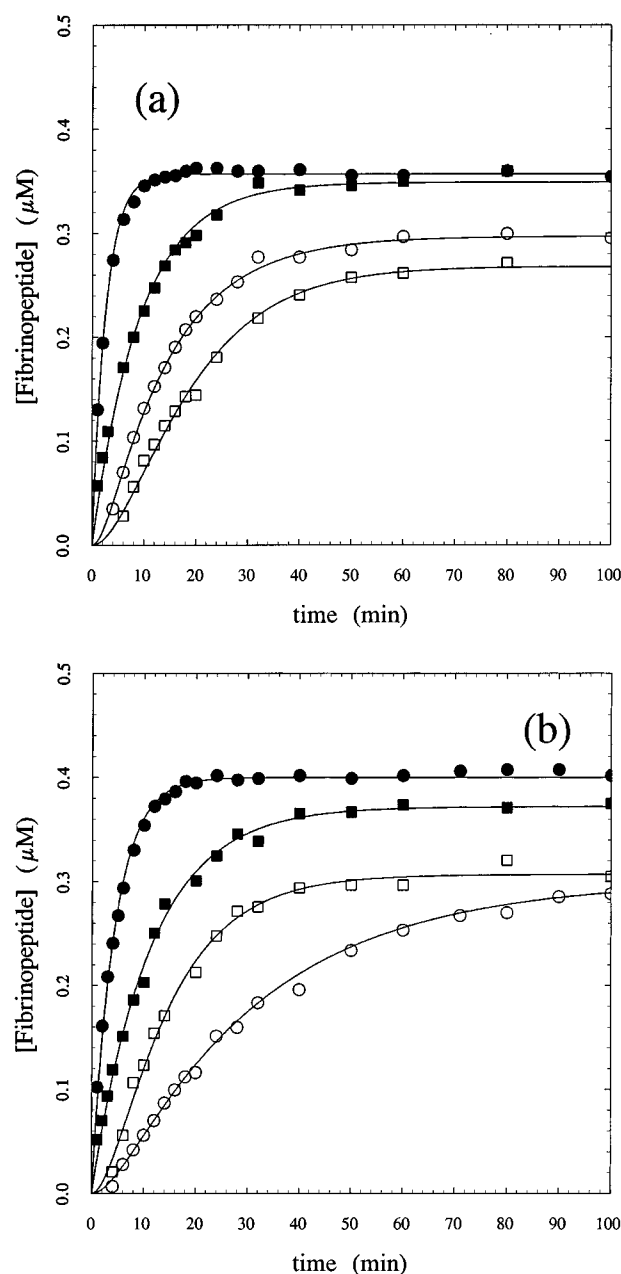


FIGURE 3: Progress curves of FpA (● and ■) and FpB (○ and □) release by the slow and fast forms of thrombin as a function of time. Experimental conditions were as follows: 0.2  $\mu\text{M}$  fibrinogen, 5 mM Tris, 0.1% PEG, pH 8.0, 45 °C (● and ○) or 5 °C (□ and ■), and 0.2 M NaCl (a) or 0.2 M ChCl (b). Continuous lines were drawn according to eqs 3a,b in the text, with best-fit parameter values for  $k_{cat}/K_m$  shown in Figure 4. The values of  $e_T$ ,  $[\text{FpA}]_\infty$ , and  $f$  in the various conditions were, respectively, as follows: 0.391 nM,  $0.349 \pm 0.004 \mu\text{M}$ , and  $0.833 \pm 0.008$  (NaCl, 5 °C); 2.0 nM,  $0.372 \pm 0.004 \mu\text{M}$ , and  $0.753 \pm 0.009$  (ChCl, 5 °C); 0.8 nM,  $0.357 \pm 0.001 \mu\text{M}$ , and  $0.77 \pm 0.02$  (NaCl, 45 °C); and 5.865 nM,  $0.400 \pm 0.001 \mu\text{M}$ , and  $0.83 \pm 0.01$  (ChCl, 45 °C). Note the lower asymptotic value for the release of FpB due to loss during centrifugation of the sample prior to HPLC analysis (see Materials and Methods).

dissociation into the parent species and the reaction proceeds rapidly toward the acylation step, followed by deacylation and dissociation of FpA and fibrin I. The higher activation energy associated with fibrinogen dissociation makes the value of  $\alpha$  decrease significantly in the temperature range of physiological interest around 37 °C. This explains the marked deviation from linearity in the plot in Figure 4. The parameter  $\alpha$  drops to about 0.5 at 37 °C but still indicates a

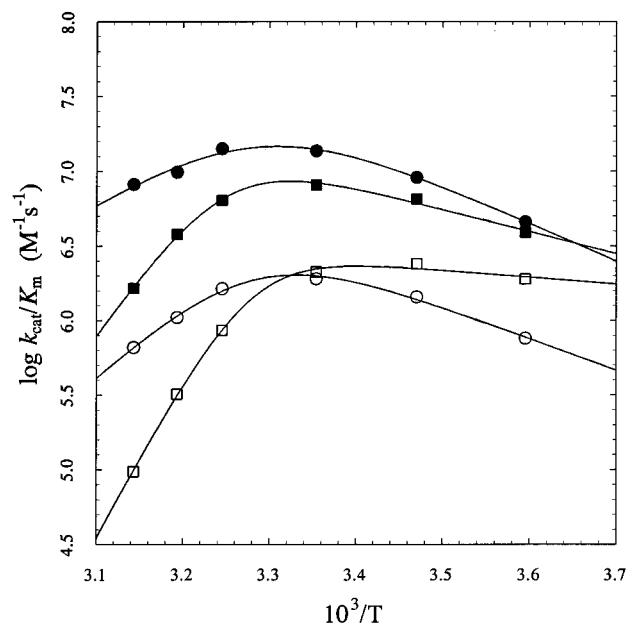


FIGURE 4: Arrhenius plots of the specificity constants for FpA (○ and ●) and FpB (□ and ■) release by the slow and fast forms of thrombin in the temperature range from 5 to 45 °C. Experimental conditions were as follows: 5 mM Tris, 0.1% PEG, pH 8.0, and 0.2 M NaCl for the fast form (● and ■) or 0.2 M ChCl for the slow form (○ and □). Continuous lines were drawn according to eq 7 in the text, with best-fit parameter values listed in Table 2.

Table 2: Kinetic Parameters for the Interaction of the Slow and Fast Forms of Thrombin with Fibrinogen and Fibrin I, Leading to Release of FpA and FpB

	$k_{1,0}$ ( $\mu\text{M}^{-1} \text{s}^{-1}$ )	$\alpha_0$	$E_1$ (kcal/mol)	$E_a$ (kcal/mol)
Fast form:				
FpA	$19 \pm 4$	$3 \pm 2$	$12 \pm 2$	$28 \pm 3$
FpB	$9.1 \pm 0.7$	$11 \pm 4$	$6.8 \pm 0.9$	$45 \pm 3$
Slow form:				
FpA	$2.5 \pm 0.3$	$4 \pm 1$	$10 \pm 1$	$34 \pm 2$
FpB	$2.5 \pm 0.2$	$7 \pm 2$	$2.1 \pm 0.9$	$51 \pm 2$

significant degree of stickiness of fibrinogen. The combination of a diffusion-controlled encounter and a rate constant for acylation comparable to that for dissociation into the parent species contributes to the optimization of the kinetic mechanism of recognition and hydrolysis of this thrombin substrate. Fibrin I shows some noteworthy differences compared to fibrinogen. The second-order rate constant is again faster in the fast form, although the value is slightly slower than that of fibrinogen. The activation energy for formation of the Michaelis–Menten complex is significantly smaller than that observed for fibrinogen, indicating that there is practically no barrier, other than diffusion, opposing the interaction of fibrin I with thrombin. The stickiness of fibrin I is considerably more pronounced, again independent of the allosteric state of thrombin. The activation energy associated with the parameter of stickiness is 17 kcal/mol higher than that of fibrinogen. At 37 °C, however, the value of  $\alpha$  becomes 0.6, which is comparable to that seen for fibrinogen.

In view of the findings from the temperature dependent studies, the origin of the low energy barrier for formation of the enzyme–substrate complex was investigated further. A possible origin of this effect can be found in the electrostatic steering that may help orient the enzyme and the substrate for optimal formation of the complex. The electrostatic properties of thrombin are quite peculiar and

pronounced, due to the presence of several charged residues in the domain responsible for recognition of fibrinogen (Martin et al., 1992; Stubbs et al., 1992). Indeed, electrostatic steering has been shown to play an important role in the interaction of thrombin with hirudin (Karshikov et al., 1992). The salt dependence of the specificity constant for the release of FpA and FpB was studied over the concentration range from 100 to 800 mM, and the results are shown in Figure 5. Again, the Shafer mechanism was found to be obeyed under all conditions examined, regardless of the nature of the salt and its concentration. The results obey a straight line in the plot from which the value of  $\Gamma_{\text{salt}}$  can be estimated directly. This value is independent of the allosteric state of the enzyme and is about  $-1.6$  for FpA and  $-2.5$  for FpB. The marked differences between the two fibrinopeptides indicate differences in ionic contributions to formation of the transition state for fibrinogen and fibrin I. These contributions may include specific ion binding interactions with thrombin and fibrinogen or fibrin I, as well as nonspecific electrostatic effects. In the salt concentration range studied, monovalent cation effects can be ruled out in the case of thrombin since  $\text{Ch}^+$  is too bulky to bind to the enzyme and  $\text{Na}^+$  binding has a  $K_d = 22$  mM (Wells & Di Cera, 1992) which depends only weakly on ionic strength (E. R. Guinto and E. Di Cera, in preparation). Furthermore, no difference in  $\Gamma_{\text{salt}}$  is detected when  $\text{Na}^+$  is replaced by  $\text{Ch}^+$ , also excluding preferential binding of  $\text{Na}^+$  to fibrinogen or fibrin I. A possible competitive inhibition of the formation of the transition state by  $\text{Cl}^-$  was considered. This possibility is borne out by the well documented inhibition of hirudin binding to thrombin by this anion (Ayala & Di Cera, 1994), which has however no effect on the hydrolysis of small chromogenic substrates (Wells & Di Cera, 1992). The structural origin of the effect is likely provided by binding of  $\text{Cl}^-$  to the positively charged region of the fibrinogen binding loop (Martin et al., 1992; Stubbs et al., 1992). Hirudin binding is opposed by  $\text{Cl}^-$  binding to a single site (Ayala & Di Cera, 1994), an effect too small to account for the values of  $\Gamma_{\text{salt}} < -1$  shown in Figure 5. However, a contribution from fibrinogen or fibrin I to the observed salt effects cannot be ruled out. Hence, the role of nonspecific electrostatic components in the formation of the transition state was examined by studies of the salt dependence of the interactions in NaF. The anion  $\text{F}^-$  has a higher hydration energy compared to  $\text{Cl}^-$  (Suelter, 1974; Collins & Washabaugh, 1985; Collins, 1995), which reduces the likelihood of its binding specifically to thrombin, fibrinogen, or fibrin I. The results of the studies carried out in the presence of NaF are also given in Figure 5. The presence of  $\text{F}^-$  has no effect on the value of  $\Gamma_{\text{salt}}$ , implying that an important driving force for the formation of the thrombin–fibrinogen and thrombin–fibrin I complexes comes from electrostatic coupling. Electrostatic effects are more pronounced for the release of FpB. The differences in the values of specificity constants observed between NaCl and NaF are conducive to the existence of specific binding interactions of  $\text{Cl}^-$  to the enzyme, but the similarity of the slopes of the data in Figure 5 suggests that specific anion effects make only a small contribution to the destabilization of the transition state, with most of the effect being dominated by electrostatic screening of the charged species involved in the recognition process.

While the effect of NaF on the release of fibrinopeptides was being studied, a drastic difference in the size and

Table 3: Phenomenological Parameters for the Salt-Dependence of the Interaction of Thrombin with Fibrinogen and Fibrin I, Leading to Release of FpA and FpB

	NaCl	ChCl	NaF	NaCl	ChCl	NaF
$A_0$	$6.08 \pm 0.04$	$5.08 \pm 0.05$	$6.58 \pm 0.04$	$5.30 \pm 0.07$	$4.65 \pm 0.05$	$6.00 \pm 0.06$
$\Gamma_{\text{salt}}$	$-1.58 \pm 0.07$	$-1.68 \pm 0.08$	$-1.50 \pm 0.08$	$-2.43 \pm 0.09$	$-2.35 \pm 0.07$	$-2.40 \pm 0.09$
	FpA			FpB		

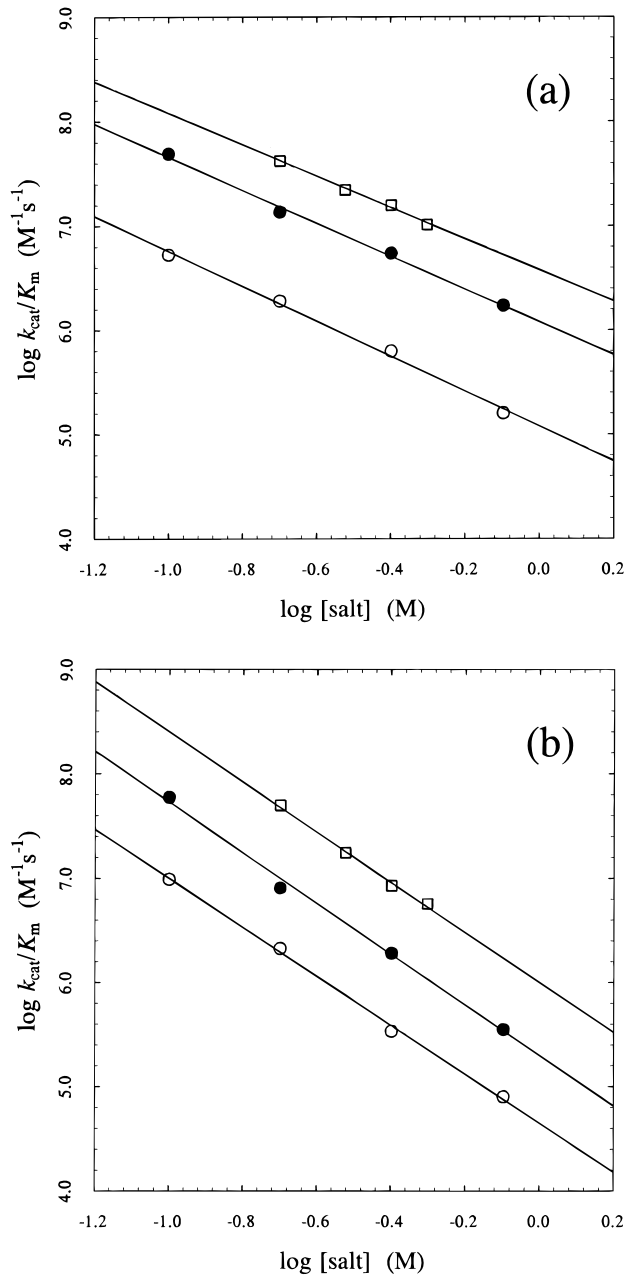


FIGURE 5: Effect of salt concentration on the specificity constant for the release of FpA (a) and FpB (b). Experimental conditions were as follows: 5 mM Tris, 0.1% PEG, pH 8.0, and in the presence of NaCl (●), ChCl (○), or NaF (□). Continuous lines were drawn according to eq 8 in the text, with best-fit parameter values listed in Table 3.

turbidity of the clot was observed. This prompted investigation of the role of  $\text{Na}^+$  and  $\text{Cl}^-$  on fibrin polymerization. Salt effects on fibrin polymerization have been documented for a long time (Ferry & Morrison, 1947; Shulman et al., 1953; Latallo et al., 1962; Weisel, 1986; Nair et al., 1986; Kaminski et al., 1991), but they have been interpreted in terms of ionic strength effects, without any attempt to assess

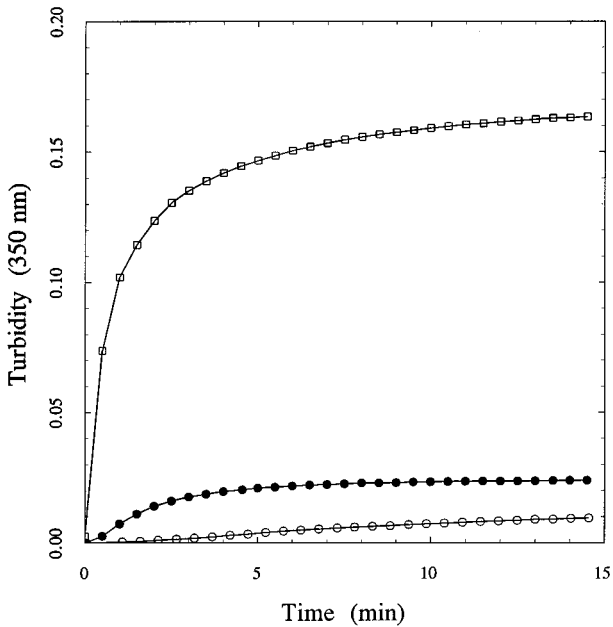


FIGURE 6: Clotting curves measured as changes in turbidity at 350 nm as a function of time. Experimental conditions were as follows: 4 nM thrombin, 0.25  $\mu\text{M}$  fibrinogen, 5 mM Tris, 0.1% PEG, pH 8.0, 25  $^\circ\text{C}$ , and in the presence of NaCl (●), ChCl (○), or NaF (□). Note the drastic difference in the clotting curve obtained in NaF. The clotting time is 20 s (NaCl), 150 s (ChCl), or 2 s (NaF).

the role of possible specific ion binding interactions. Ferry was the first to report that an increase in ionic strength lowers the turbidity of the fibrin clot and induced a transition from a coarse to a fine clot (Ferry & Morrison, 1947). In his original experiments, and in practically all subsequent studies, the ionic strength was changed with NaCl or other salts containing  $\text{Cl}^-$ . This prompted us to look for specific effects due to this anion. Clotting curves were measured in the presence of 200 mM NaCl, ChCl, or NaF. The results are shown in Figure 6 as changes in turbidity at 350 nm as a function of time. Comparison of clotting curves in NaCl and ChCl shows that the presence of  $\text{Na}^+$  reduces the lag time for clot formation, as already reported (Mathur et al., 1993), and has a small effect on the equilibrium value of turbidity. This value is an important indicator of the size of the fibers formed in the clot (Carr & Hermans, 1978; Hantgan & Hermans, 1979; Weisel, 1986). The delayed formation of the clot is most likely due to thrombin being in its slow form in ChCl. The difference in clotting time between NaCl and ChCl estimated from the inflection point of the progress curve (De Cristofaro & Di Cera, 1991) is consistent with the difference in the value of  $k_{\text{cat}}/K_m$  for the two forms of thrombin. Comparison of clotting curves in NaCl and NaF shows that the presence of  $\text{Cl}^-$  drastically affects both the clotting time and the size of fibers formed, with the equilibrium value of turbidity decreasing more than 10-fold compared to that in NaF. The delayed formation of the clot in NaCl compared to that in NaF is not accounted for by the

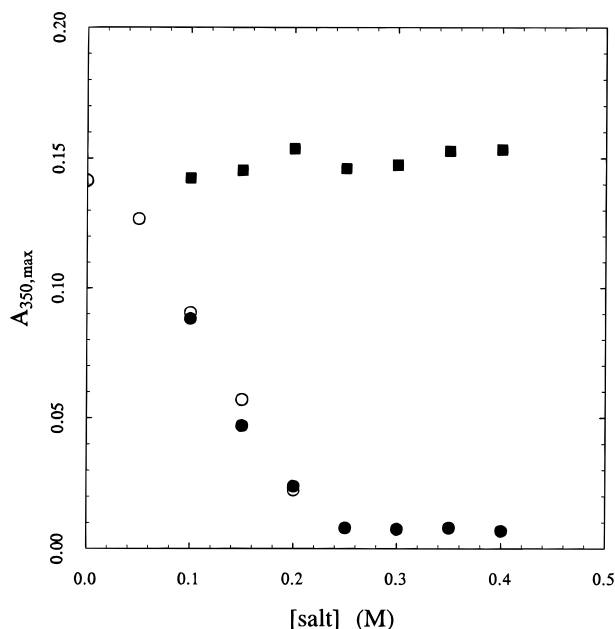


FIGURE 7: Equilibrium value of turbidity at 350 nm for clotting curves obtained as a function of salt concentration under the following experimental conditions: 4 nM thrombin, 0.25  $\mu$ M fibrinogen, 5 mM Tris, 0.1% PEG, pH 8.0, 25  $^{\circ}$ C, and in the presence of NaCl (●) or NaF (■). The change in  $A_{350,\text{max}}$  depends solely on the concentration of  $\text{Cl}^-$ , as also demonstrated by the values obtained at constant ionic strength (200 mM) where NaCl is replaced by NaF (○).

difference in  $k_{\text{cat}}/K_m$  observed in NaCl and NaF (see Figure 5), which is only a factor of 2, implying that the clotting time is not always related to the steps preceding polymerization, contrary to previous suggestions (Hantgan & Hermans, 1979; De Cristofaro & Di Cera, 1991). The drastic effect seen on the equilibrium value of turbidity is entirely due to an effect on the ensuing polymerization that develops into thinner fibers and a finer clot when  $\text{Cl}^-$  is present. Thrombin bound to fibrin is known to have interesting enzymatic properties toward fibrinogen and other physiologically important components (Liu et al., 1979; Kaminsky & McDonagh, 1988; Kaminsky et al., 1991; Naski & Shafer, 1990, 1991), but it is unlikely that this would cause a 10-fold increase in turbidity in the clotting curve. The difference between clots formed in NaCl and NaF echoes that seen at high and low ionic strengths by others (Ferry & Morrison, 1947; Nair et al., 1986; Kaminski et al., 1991), which suggests that the ionic strength effect on fibrin polymerization reported previously is instead a very specific effect of  $\text{Cl}^-$ . The role of  $\text{Cl}^-$  in controlling the size of the fibers in the fibrin gel was quantified by measurements of the equilibrium value of turbidity as a function of salt concentration. The results are shown in Figure 7. In the salt concentration range from 100 to 400 mM, there is no effect of NaF, while increasing the NaCl concentration leads to a drastic decrease in the equilibrium value of turbidity. The effect is due entirely to  $\text{Cl}^-$  and not to  $\text{Na}^+$  or a change in ionic strength. In fact, when similar measurements are carried out at a constant ionic strength (200 mM) by replacement of NaCl with NaF, the results are practically identical to those derived by changing the [NaCl] alone. The equilibrium value of turbidity depends solely on the concentration of  $\text{Cl}^-$  ions present in solution.

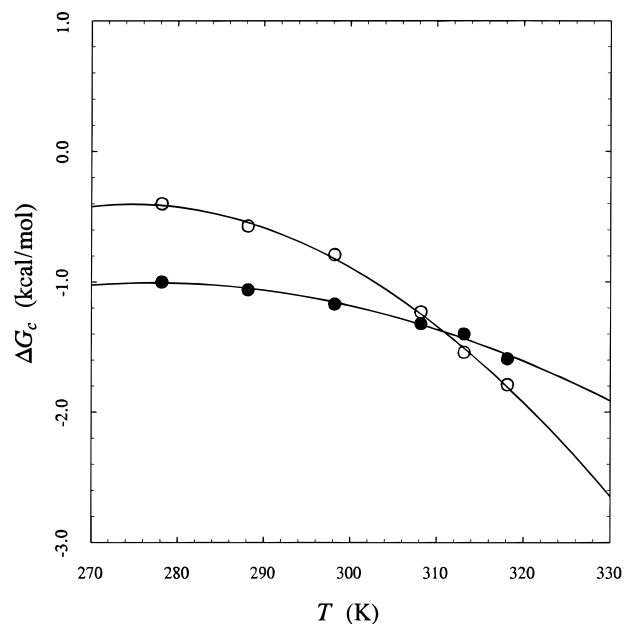


FIGURE 8: Effect of temperature on the coupling free energy for the slow  $\rightarrow$  fast transition of thrombin. Data refer to FpA (●) or FpB (○). The value of  $\Delta G_c = -RT \ln(s_1/s_0)$ , where  $s$  denotes the  $k_{\text{cat}}/K_m$  ratio for the slow ( $s_0$ ) and fast ( $s_1$ ) forms (Guinto et al., 1995), decreases with increasing  $T$ . The slope in the plot measures  $-\Delta S_c$  and indicates that entropy drives the preferential interaction of fibrinogen or fibrin I with the fast form of thrombin, as recently reported for hirudin binding (Ayala et al., 1995).

## DISCUSSION

The interaction of thrombin with fibrinogen and fibrin I is dominated by two driving forces: electrostatic coupling and the conformational state of thrombin. The difference  $E_1 - E_a$  provides an upper bound for the enthalpy of binding. This term is on the order of  $-20$  kcal/mol for fibrinogen and  $-50$  kcal/mol for fibrin I, regardless of the allosteric state of thrombin. The drastic difference between the two substrates represents strong, albeit indirect, evidence that FpA is released from a molecule that is very different from the substrate for FpB release, as implied by the sequential mechanism of Shafer (Higgins et al., 1983; Lewis et al., 1985). Molecular recognition of fibrin I is enthalpically favored over fibrinogen, signaling the involvement of a larger surface area and perhaps hydrophobic effect (Ayala et al., 1995). Due to the similar binding affinities of fibrinogen (Hopfner & Di Cera, 1992) and fibrin I (Liu et al., 1979; Kaminsky & McDonagh, 1988; Naski & Shafer, 1990), it follows that the entropic loss upon binding of fibrin I must also be larger than that observed upon binding of fibrinogen.

The temperature studies reveal important information on the origin of preferential interaction of fibrinogen and fibrin I with the fast form of thrombin. Using the approach developed recently for the analysis of thrombin–hirudin interaction (Ayala et al., 1995) and site-directed mutations of thrombin (Di Cera, 1995; Guinto et al., 1995), the coupling free energy for allosteric switching,  $\Delta G_c$ , can be measured from the ratio of the specificity constants of the fast and slow forms. The values of  $\Delta G_c$  obtained as a function of temperature are shown in Figure 8. The slope in the plot gives the value of  $-\Delta S_c$ . The coupling entropy is positive throughout the temperature range studied and so is the enthalpy of coupling. The coupling free energy is negative in the same range, indicating preferential interaction with



the fast form. Hence, the origin of this preferential interaction is entropic. Enthalpic components stabilize binding of fibrinogen and fibrin I to the slow form in the transition state, while entropic components favor binding to the fast form. In the temperature range of physiological interest, the entropic components predominate and give rise to preferential binding to the fast form. This result echoes the scenario for the thrombin–hirudin interaction, where preferential binding of hirudin to the fast form was found to be entropic (Ayala et al., 1995). The curvature in the plot in Figure 8 is not necessarily due to a heat capacity change in the allosteric switching, because it is consistent with eq 5 applied to the slow and fast forms and is fully explained by a change in the stickiness of the substrate over the temperature range examined.

In addition to the enthalpic and entropic components, differences in recognition of fibrinogen and fibrin I by thrombin are evident from the salt dependence of the specificity constants for the release of FpA and FpB. Although the specificity changes in different salts, the slope of the plot is independent of the salt used. This effect is noteworthy, in view of the possible mechanistic interpretation of  $\Gamma_{\text{salt}}$ . The slope in the plot in Figure 5 can be interpreted in terms of the preferential interaction of the cation and anion components of each salt with thrombin, the substrate, and the thrombin–substrate complex in the transition state. However, there are some serious problems with this interpretation. Cations like  $\text{Na}^+$  and  $\text{Ch}^+$  have widely different hydration energies and ionic radii (Suelter, 1974; Collins & Washabaugh, 1985; Collins, 1995), which makes it unlikely that they interact equally with macromolecular components like thrombin, fibrinogen, and fibrin I. The  $\text{Na}^+$  binding site of thrombin is too narrow to accommodate  $\text{Ch}^+$  (Di Cera et al., 1995), and valence screening (Nayal & Di Cera, 1994) of over 20 crystal structures confirms the  $\text{Na}^+$  specificity of thrombin (Nayal & Di Cera, 1996). Likewise,  $\text{Cl}^-$  and  $\text{F}^-$  differ widely in ionic radii and hydration energies (Collins, 1995), with  $\text{F}^-$  behaving typically as an “inert” anion with a small tendency to interact with macromolecular components, unlike the less hydrated  $\text{Cl}^-$ . Hence, in the presence of ion binding interactions,  $\Gamma_{\text{salt}}$  should be significantly different in NaCl, ChCl, and NaF. The similarities in the slopes shown in Figure 5 suggest a different interpretation of  $\Gamma_{\text{salt}}$  in terms of the electrostatic coupling between thrombin and the substrate that is screened nonspecifically by the charged ions in solution. The differences in specificity constants reported in Figure 5 are therefore due to specific binding interactions of  $\text{Na}^+$  and presumably  $\text{Cl}^-$  with thrombin and the substrate, but the slope in the plot is related more directly to the electrostatic contribution to the formation of the transition state.

In the case of  $\text{Na}^+$ , crystallographic analysis provides unequivocal evidence of a specific binding interaction with thrombin (Di Cera et al., 1995). Functional studies provide overwhelming support for the existence of a  $\text{Na}^+$ -induced conformational change of the enzyme (Wells & Di Cera, 1992; Ayala & Di Cera, 1994; Ayala et al., 1995; Dang et al., 1995; Di Cera et al., 1995). Specific binding of  $\text{Cl}^-$  to thrombin has been suggested to occur at the fibrinogen recognition site (Ayala & Di Cera, 1994), although no evidence of absorbed anions at this site can be found crystallographically (Rydel et al., 1991). In the case of fibrinogen and fibrin I, no structural information is available.

The slow and fast forms of thrombin recognize fibrinogen and the fibrin I monomer with different specificity, as a result of the  $\text{Na}^+$ -induced conformational change. In both forms, however, the specificity can be reduced to the same extent by an increase in the salt concentration due to a nonspecific screening effect of the counterions on the charged residues of thrombin and the substrates participation in the formation of the transition state. This explains the similar  $\Gamma_{\text{salt}}$  values in NaCl and ChCl. Binding of  $\text{Cl}^-$  to thrombin and/or the substrate also affects specificity, presumably through a conformational change or a competitive effect. However, the replacement of  $\text{Cl}^-$  with  $\text{F}^-$  does not result in a change in  $\Gamma_{\text{salt}}$  since the electrostatic screening effect predominates when the salt concentration is being increased. The value of  $\Gamma_{\text{salt}}$  is larger in the case of FpB release, suggesting that electrostatic effects are more pronounced in the thrombin–fibrin I interaction than in the thrombin–fibrinogen interaction. The release of FpA unmasks polymerization sites in fibrin I, and the release of FpB occurs after formation of protofibrils. It is possible that the ensuing polymerization locally decreases the electrostatic potential at the recognition site for the enzyme, thereby increasing the electrostatic coupling with the positively charged region of the fibrinogen recognition site.

The molecular picture emerging from these studies is that electrostatic steering provides a mechanism for recognition of fibrinogen and fibrin I by thrombin, favoring the correct orientation of the components for formation of a productive complex. This driving force accounts for the low energy barrier to the encounter and the diffusion-controlled nature of the interaction. Once the complex in the transition state is formed, the enzyme shifts to the fast form due to its higher specificity, this shift being driven by entropic factors. By analogy with thrombin–hirudin interaction, the entropy-driven allosteric switch may result from the contribution of the hydrophobic effect (Ayala et al., 1995). Hence, electrostatic forces would guide the formation of the transition state, while hydrophobic components would optimize recognition once the transition state is formed. This scenario finds much support from structural studies, given that binding to the fibrinogen recognition site of thrombin involves many polar and hydrophobic interactions (Rydel et al., 1991).

The importance of  $\text{Cl}^-$  in the polymerization steps leading to clot formation is documented here for the first time. The effect of  $\text{Cl}^-$  on fibrin polymerization and the size of the fibrin fibers has been interpreted previously as an effect of ionic strength (Ferry & Morrison, 1947; Nair et al., 1986; Kaminski et al., 1991). A drastic enhancement is seen in the equilibrium turbidity of the clotting curve in NaF, compared to a solution containing NaCl. There is a specific binding interaction of  $\text{Cl}^-$  to the fibrin polymer that affects the size of the fibers and eventually determines the fine or coarse nature of the clot. It is an increase in the concentration of  $\text{Cl}^-$ , and not the ionic strength, that converts the coarse into a fine clot. The two most abundant ions in the blood participate in crucial aspects of blood coagulation.  $\text{Na}^+$  increases the fraction of thrombin in the procoagulant fast form, while  $\text{Cl}^-$  reduces the thickness of the fibrin fibers in the developing clot. Both effects are large and physiologically important and certainly play a key role in the pathogenesis of thrombosis. Clots formed in high concentrations of NaCl, as seen in several pathological conditions (Ratnoff & Forbes, 1991), develop fast and involve thin

fibers. Clots formed in low concentrations of NaCl develop slowly but lead to thick fibers.

## REFERENCES

- Ayala, Y. M., & Di Cera, E. (1994) *J. Mol. Biol.* 235, 733–746.
- Ayala, Y. M., Vindigni, A., Nayal, M., Spolar, R. S., Record, M. T., Jr., & Di Cera, E. (1995) *J. Mol. Biol.* 254, 787–798.
- Barshop, B. A., Wrenn, R. F., & Frieden, C. (1983) *Anal. Biochem.* 130, 134–145.
- Binnie, C. G., & Lord, S. T. (1993) *Blood* 81, 3186–3192.
- Carr, M. E., Jr., & Hermans, J. (1978) *Macromolecules* 11, 46–50.
- Cleland, W. W. (1977) *Adv. Enzymol. Relat. Areas Mol. Biol.* 45, 237–387.
- Collins, K. D. (1995) *Proc. Natl. Acad. Sci. U.S.A.* 92, 5553–5557.
- Collins, K. D., & Washabaugh, M. W. (1985) *Q. Rev. Biophys.* 18, 323–422.
- Dang, Q. D., & Di Cera, E. (1994) *J. Protein Chem.* 13, 367–373.
- Dang, Q. D., Vindigni, A., & Di Cera, E. (1995) *Proc. Natl. Acad. Sci. U.S.A.* 92, 5977–5981.
- De Cristofaro, R., & Di Cera, E. (1991) *J. Protein Chem.* 10, 455–468.
- De Cristofaro, R., & Di Cera, E. (1992) *Biochemistry* 31, 257–265.
- Di Cera, E. (1995) *Thermodynamic Theory of Site Specific Binding Processes in Biological Macromolecules*, Cambridge University, U.K.
- Di Cera, E., Guinto, E. R., Vindigni, A., Dang, Q. D., Ayala, Y., Wuyi, M., & Tulinsky, A. (1995) *J. Biol. Chem.* 270, 22089–22092.
- Doolittle, R. F. (1984) *Annu. Rev. Biochem.* 53, 195–236.
- Ferry, J. D., & Morrison, P. R. (1947) *J. Am. Chem. Soc.* 69, 388–399.
- Guinto, E. R., Vindigni, A., Ayala, Y., Dang, Q. D., & Di Cera, E. (1995) *Proc. Natl. Acad. Sci. U.S.A.* 92, 22089–22092.
- Hageman, T. C., & Scheraga, H. A. (1974) *Arch. Biochem. Biophys.* 164, 707–715.
- Hantgan, R. R., & Hermans, J. (1979) *J. Biol. Chem.* 254, 11272–11281.
- Higgins, D. L., Lewis, S. D., & Shafer, J. A. (1983) *J. Biol. Chem.* 258, 9276–9282.
- Hofsteenge, J., Taguchi, H., & Stone, S. R. (1986) *Biochem. J.* 237, 243–251.
- Hopfner, K.-P., & Di Cera, E. (1992) *Biochemistry* 31, 11567–11571.
- Kaminski, M., & McDonagh, J. (1988) *J. Biol. Chem.* 258, 10530–10535.
- Kaminski, M., Siebenlist, K. R., & Mosesson, M. W. (1991) *J. Lab. Clin. Med.* 117, 218–225.
- Karshikov, A., Bode, W., Tulinsky, A., & Stone, S. R. (1992) *Protein Sci.* 1, 727–735.
- Kenar, K. T., Garcia-Moreno, B., & Freire, E. (1995) *Protein Sci.* 4, 1934–1938.
- Latallo, Z. S., Fletcher, A. P., Alkjaersig, N., & Sherry, S. (1962) *Am. J. Physiol.* 202, 675–680.
- Lewis, S. D., Shields, P. P., & Shafer, J. A. (1985) *J. Biol. Chem.* 260, 10192–10199.
- Liu, C. Y., Nossel, H. L., & Kaplan, K. L. (1979) *J. Biol. Chem.* 254, 10421–10425.
- Lord, S. T., Rooney, M. M., Hopfner, K.-P., & Di Cera, E. (1995) *J. Biol. Chem.* 270, 24790–24793.
- Lu, M., & Draper, D. E. (1994) *J. Mol. Biol.* 244, 572–585.
- Martin, P. D., Robertson, W., Turk, D., Huber, R., Bode, W., & Edwards, B. F. P. (1992) *J. Biol. Chem.* 267, 7911–7920.
- Martinelli, R. A., & Scheraga, H. A. (1980) *Biochemistry* 19, 2343–2350.
- Mathur, A., Schlapkohl, W. A., & Di Cera, E. (1993) *Biochemistry* 32, 7568–7573.
- Mihalyi, E. (1988) *Biochemistry* 27, 976–982.
- Mihalyi, E., Tercero, J. C., & Diaz-Mauriño, T. (1991) *Biochemistry* 30, 4753–4762.
- Nair, C. H., Shah, G. A., & Dhall, D. P. (1986) *Thromb. Res.* 42, 809–816.
- Naski, M. C., & Shafer, J. A. (1990) *J. Biol. Chem.* 265, 1401–1407.
- Naski, M. C., & Shafer, J. A. (1991) *J. Biol. Chem.* 266, 13003–13010.
- Nayal, M., & Di Cera, E. (1994) *Proc. Natl. Acad. Sci. U.S.A.* 92, 817–821.
- Nayal, M., & Di Cera, E. (1996) *J. Mol. Biol.* 256, 228–234.
- Ng, A. S., Lewis, S. D., & Shafer, J. A. (1993) *Methods Enzymol.* 222, 341–358.
- Overman, L. B., & Lohman, T. M. (1994) *J. Mol. Biol.* 236, 165–178.
- Ratnoff, O. D., & Forbes, C. D. (1991) *Disorders of Hemostasis*, Saunders, Philadelphia, PA.
- Record, M. T., Jr., & Anderson, C. F. (1995) *Biophys. J.* 68, 786–794.
- Record, M. T., Jr., Anderson, C. F., & Lohman, T. M. (1978) *Q. Rev. Biophys.* 11, 103–178.
- Rydell, T. J., Tulinsky, A., Bode, W., & Huber, R. (1991) *J. Mol. Biol.* 221, 583–601.
- Shulman, S., Katz, S., & Ferry, J. D. (1953) *J. Gen. Physiol.* 36, 759–766.
- Stoll, V. S., & Blanchard, J. S. (1990) *Methods Enzymol.* 182, 24–38.
- Stubbs, M., Oschkinat, H., Mayr, I., Huber, R., Anglikar, H., Stone, S. R., & Bode, W. (1992) *Eur. J. Biochem.* 206, 187–195.
- Sturtevant, J. M., Laskowski, M., Donnelly, T. H., & Scheraga, H. A. (1955) *J. Am. Chem. Soc.* 77, 6168–6172.
- Suelter, C. H. (1974) in *Metal Ions in Biological Systems*, Marcel Dekker, New York.
- von Hippel, P. H., & Wong, K. Y. (1965) *J. Biol. Chem.* 240, 3909–3923.
- Weisel, J. W. (1986) *Biophys. J.* 50, 1079–1093.
- Wells, C. M., & Di Cera, E. (1992) *Biochemistry* 31, 11721–11730.
- Wilf, J., & Minton, A. P. (1986) *Biochemistry* 25, 3124–3133.
- Zimmerle, C. T., & Frieden, C. (1989) *Biochem. J.* 258, 381–387.

BI952834D